Journal of Mammalian Evolution
https://doi.org/10.1007/s10914-020-09498-6

ORIGINAL PAPER

Shoulder Muscle Architecture in the Echidna (Monotremata: *Tachyglossus aculeatus*) Indicates Conserved Functional Properties

Sophie Regnault[1] · Philip Fahn-Lai[1] · Rachel M. Norris[2] · Stephanie E. Pierce[1]

Abstract

Monotremes are a group of egg-laying mammals, possessing a mosaic of ancestral and derived anatomical features. Despite much interest in monotremes from phylogenetic, morphological, and ecological perspectives, they have been the subject of relatively few biomechanical studies. In this study, we examined shoulder and proximal forelimb muscle anatomy and architecture in the short-beaked echidna, *Tachyglossus aculeatus*, through contrast-enhanced computed tomography and gross dissection. Muscle architecture is a major determinant of muscle function and can indicate specialized muscle roles, such as the capacity for generating large forces (through large physiological cross-sectional area, PCSA) or working ranges (through long fascicle lengths). We hypothesized that some muscles would exhibit architectural specializations convergent with other fossorial and/or sprawling animals, and that other muscles would reflect the echidna's unusual anatomy and locomotor style. Instead, we found the shoulder and proximal forelimb muscles in echidna to have little variation in their architecture. The muscles generally had long fascicles and small-to-intermediate PCSAs, consistent with force production over a wide working range. Further, muscles did not show overt differences in architecture that, in therian mammals, have been linked to increased forelimb mobility and the transition from sprawling to parasagittal posture. Our measures of architectural disparity placed the echidna closer to the tegu lizard than other sprawling fossorial mammals (e.g., mole). The low architectural diversity found in the echidna's shoulder and proximal forelimb muscles is interpreted as a lack of functional specialization into distinct roles. We hope our study will contribute to greater understanding of monotreme anatomy and biomechanical function, and to the reconstruction of musculoskeletal evolution in mammals.

Keywords DiceCT · Forelimb evolution · Biomechanics · Muscle function · Limb posture · Mammal

Introduction

Echidnas (Tachyglossidae) represent only one of two living families of Monotremata, an early-diverging lineage of egg-laying mammals. Generally classified as fossorial specialists, echidnas possess robust pectoral girdle and limb bones, a broad manus, and long, spade-like claws (Augee et al. 2006). However, within the forelimb they also display many anatomical features reminiscent of earlier mammalian relatives (Luo 2015; Regnault and Pierce 2018). These include additional bones within the pectoral girdle (an interclavicle fused with the clavicle, a coracoid fused to the scapula, and an epicoracoid), a laterally-facing hemi-sellar glenoid, lack of a scapular spine, and similar general humeral morphology (Luo 2015; Gambaryan et al. 2015; see also Fig. 1). Although the subject of few biomechanical studies (Jenkins 1970; Gambaryan and Kuznetsov 2013; Clemente et al. 2016), their unusual anatomy and phylogenetic placement makes musculoskeletal function in echidnas of particular interest. Not only can they offer an independent case study on how anatomy is shaped by evolutionary adaptation and constraint, but they can also provide insight on the evolution of the mammalian musculoskeletal system and ancestral mammalian function.

Echidnas have a characteristic sprawling gait, with rolling of the trunk and a slow, pace-like walk (Gambaryan and Kuznetsov 2013; Clemente et al. 2016). Walking kinematics show long-axis rotation to be the principal motion of the

Electronic supplementary material The online version of this article (https://doi.org/10.1007/s10914-020-09498-6) contains supplementary material, which is available to authorized users.

✉ Stephanie E. Pierce
spierce@oeb.harvard.edu

[1] Museum of Comparative Zoology and Department of Organismic and Evolutionary Biology, Harvard University, 26 Oxford Street, Cambridge, MA, USA

[2] School of Animal and Veterinary Science, The University of Adelaide, Roseworthy Campus, Roseworthy, South Australia 5371, Australia

Published online: 14 March 2020

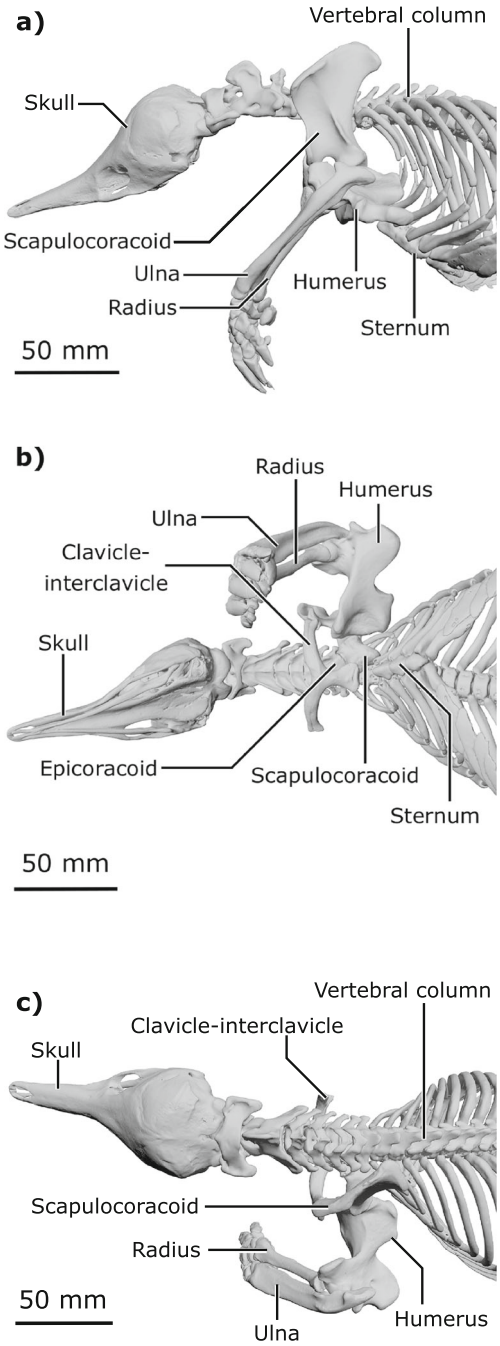

Fig. 1 Rendering of the skeleton of the short-beaked echidna *Tachyglossus aculeatus* produced from μCT scans of specimen SEP42 (Regnault and Pierce 2018) before contrast-staining, shown in **a**) left lateral view, **b**) ventral view, and **c**) dorsal view. Relevant anatomical landmarks are highlighted

humerus (Jenkins 1970), unlike most therian mammals where the predominant motion is flexion-extension within the parasagittal plane (Polly 2007), but likely similar to some earlier relatives of mammals (e.g., the non-mammalian 'pelycosaurs' and cynodonts; see Regnault and Pierce 2018). Moment arm estimations based on muscle attachment sites likewise suggest that the shoulder is optimized for internal rotation and adduction (Regnault and Pierce 2018). There appears to be little intrinsic muscular stabilization of the pectoral girdle and shoulder joints, due to the robust bony and articular morphology in monotremes (Luo 2015). However, it is unknown whether the muscles themselves are structurally specialized for the echidna's lifestyle and locomotion.

A primary determinant of muscle function is muscle architecture, or the arrangement of fibers within muscle (Lieber and Fridén 2000). Fiber length is linked to muscle shortening ability and velocity, while muscle physiological cross-sectional area (PCSA) determines how much force a muscle can generate (Lieber and Fridén 2000). Gross muscle anatomy has been described qualitatively for the echidna (Jouffroy and Lessertisseur 1971; Gambaryan et al. 2015), but muscle architecture remains unexplored in monotremes. Studies on forelimb muscle architecture of other mammals demonstrate how certain muscles have become specialized for different lifestyles and locomotion. For example, the PCSAs of m. teres major and m. subscapularis in the fossorial mole (*Scalopus aquaticus*) are disproportionately large compared to body mass (Rose et al. 2013), to produce the forceful humeral abduction and internal rotation necessary for their unusual digging style (Lin et al. 2019). The PCSA of m. subscapularis is likewise large in the fossorial badger (*Taxidea taxus*), with short fibers suggesting this muscle is specialized for stabilization of the humerus while digging (Moore et al. 2013). The PCSA of m. subscapularis is also large in the arboreal pine marten (*Martes martes*), to counteract laterally-directed reaction forces in the limb during climbing (Böhmer et al. 2018).

Here, we document the shoulder and proximal forelimb muscles and architectural parameters of the short-beaked echidna, *Tachyglossus aculeatus*, providing a detailed examination of muscle form and function in monotremes. Muscle data from the echidna are further compared to other fossorial and non-fossorial mammals, as well as sprawling non-mammals, to determine musculoskeletal specializations associated with the echidna's digging lifestyle and sprawling gait. Based on our prior work (Regnault and Pierce 2018), we predicted that the echidna would show high PCSAs for humeral adductors such as m. pectoralis (important for supporting sprawling animals during stance; e.g., Allen et al. 2010) and internal rotators such as m. teres major (important for the highly specialized fossorial mole; Rose et al. 2013). We also hypothesized convergent specializations in homologous muscles with fossorial therians (e.g., m. subscapularis). However, as many muscles differ in position, attachments, and inferred function between echidnas and therian mammals (Regnault and Pierce 2018), we further anticipated other muscles to reveal differences reflective of the echidna's mixture of plesiomorphic and derived anatomical features.

Material and Methods

Study Specimens

Four adult short-beaked echidnas (*Tachyglossus aculeatus*) were used in this study. One specimen was contrast-stained to obtain a 3D overview of whole muscle anatomy, and three specimens were dissected for architectural properties. The specimens were collected in South Australia, and provided by the University of Adelaide. Cause of death in all cases was suspected impact with a vehicle. The specimens were intact with no grossly observable injuries to the pectoral girdle/forelimb. All specimens had been collected an unknown time after death and stored frozen at −18 °C.

Whole Muscle Anatomy Via Digital Dissection

One specimen (identified as 'SEP42', body mass 3.31 kg) was scanned while frozen via micro-computed tomography (μCT) for a baseline scan to acquire skeletal morphology (scanning parameters of this specimen are detailed in Regnault and Pierce 2018). Following thawing at 4 °C, this specimen was skinned, eviscerated, and fixed in 10% neutral buffered formalin solution for one week. Following diceCT guidelines (Gignac et al. 2016), the specimen was then rinsed in deionized water and immersed in a 3% solution of Lugol's iodine for 13 weeks (1% I_2 and 2% KI *w*/*v* dissolved to a 5 L solution). The solution was agitated daily and refreshed weekly. The specimen was rinsed with deionized water and re-scanned weekly via μCT to assess the end-point of muscle staining [HMXST225 micro-CT system (X-Tek, Amherst, NH, USA); settings 130 kv, 120 mA, 2 s exposure with 1 mm copper filter, voxel size 0.11 mm] at the Harvard University Center for Nanoscale Systems.

The projections were reconstructed as a TIFF image stack using CT Pro 3D software (Nikon Metrology Inc., Brighton, MI, USA), with a beam hardening correction algorithm applied (preset option 2 within CT Pro 3D). The images were then imported into Mimics version 19.0 (Materialise, Leuven, Belgium) and the shoulder and forelimb muscles and bones on both sides of the animal manually segmented to create 3D meshes. Muscles crossing the shoulder (glenohumeral) joint were identified following the descriptions and illustrations of Gambaryan et al. (2015) and are described in Table 1. High quality bone meshes had been produced from the previous baseline scan of this specimen (Regnault and Pierce 2018), illustrated here in Fig. 1; these meshes were aligned through their anatomical landmarks with the positions of the lower quality bone meshes in the noisier post-stained scan via the "Align" tool in Mimics. The bone and muscle meshes were exported from Mimics as .stl files. Meshes were downsampled and retriangulated in Autodesk Meshmixer (Autodesk Inc., San Rafael, CA, USA). The refined bone and muscle meshes were then imported into Autodesk Mudbox (Autodesk Inc., San Rafael, CA, USA) so that specimen-specific three-dimensional models of muscles and their attachments could be generated. Muscle attachment sites were drawn onto bone models using the PTEX mapping method (see also Fahn-Lai et al. 2020).

Muscle Architecture Properties Via Physical Dissection

Three echidna specimens (body mass 2.48 kg, 2.89 kg, 3.79 kg) were thawed at 4 °C. The upper body was skinned, and muscles of the pectoral girdle and proximal forelimb identified and sequentially removed. During the dissection, exposed musculature was covered with the animal's skin, plastic wrap, and/or paper towels soaked in 0.9% phosphate-buffered saline solution to prevent dehydration. Each muscle (Table 1) was dissected free of the limb, blotted of excess moisture, weighed with an electronic scale (to the nearest 0.01 g), measured with a ruler (to the nearest mm), and photographed. Any external tendon was removed, and the muscle belly weighed and measured again. The muscle belly was incised along its length in several places to reveal the muscle fascicles; the incisions were continued following the plane of the fascicles from origin to insertion, and photographed again. The photographs were imported into ImageJ software (U.S. National Institutes of Health Bethesda, USA; Schneider et al. 2012) to measure the internal pennation angles (to nearest degree) and lengths (to nearest mm) of muscle fascicles from three different areas within the muscle, and the mean of each calculated. In one echidna specimen (SEP44; Supplementary Data file), muscle fascicles were extremely delicate and readily friable upon manipulation (suspected due to freeze-thaw cycling or the beginning of tissue autolysis); the fascicle lengths and pennation angle measurements from this specimen were excluded from the study. Tissues from the other two specimens were robust and comparable to a fresh animal.

The maximum isometric force that each muscle is capable of generating is directly proportional to its physiological cross-sectional area (PCSA). PCSA (in mm^2) was calculated using the following equation:

$$PCSA = m_M * \cos\theta / f_L * \rho \quad (1)$$

In Eq. 1, m_M denotes muscle belly mass (g), θ denotes muscle fascicle pennation angle (rad), f_L denotes muscle fascicle length (mm; functionally assumed equivalent to fiber length – see Lieber and Fridén 2000), and ρ represents the density of mammalian skeletal tissue (0.001056 gmm^{-3}; Méndez and Keys 1960).

The mean architectural parameters and PCSA were calculated for each animal's right and left sides. These values were then normalized against each animal's body mass (B_M, in grams) assuming geometric isometry ($B_M^{0.33}$ for length measurements, $B_M^{0.66}$ for PCSA, and B_M^{1} for mass measurements). A mean,

Table 1 Shoulder girdle and proximal forelimb muscles examined in this study, including their origin, insertion, and principal action on the echidna's unloaded limb

Muscle	Abbreviation	Origin	Insertion	Principal action in unloaded limb
Latissimus dorsi	LAT	Vertebral column Caudal angle of scapula	Entepicondyle of humerus	Draw scapulocoracoid medially; Humeral flexion and internal rotation
Pectoralis	PECT	Presternum and sternal elements 1–3	Major tubercle, on pectoral crest of humerus	Draw scapulocoracoid laterally; Humeral adduction, extension, and internal rotation (depending on part)
Subcoracoideus	SUBCOR	Lateral and internal surface of epicoracoid	Minor tubercle of humerus	Draw scapulocoracoid medially; Humeral flexion
Supracoracoideus	SUPCOR	Ventral surface of epicoracoid, continuing onto ventral surface of coracoid	Proximal ventral surface and major tubercle of the humerus	Draw scapulocoracoid laterally; Humeral adduction
Clavodeltoideus	CLAV-D	Ventral and cranial aspect of the clavicle and parts of the interclavicle	Proximal dorsal aspect of the humerus, along the cranial border	Draw scapulocoracoid laterally; Humeral extension and internal rotation
Acromiodeltoideus	ACR-D	Acromion process of scapula	Proximal dorsal aspect of the humerus, situated cranially	Humeral abduction and extension
Spinodeltoideus	SPN-D	Dorsal border of scapula	Proximal dorsal aspect of the humerus, along the cranial border, nested within m. clavodeltoideus	Humeral abduction and external rotation
Infraspinatus	INFSP	Infraspinous fossa on the cranial half of the scapula	Proximal dorsal aspect of humerus, adjacent to humeral head	Humeral external rotation
Supraspinatus	SUPSP	Internal surface of scapula, in the supraspinous fossa	Proximal humerus, adjacent to humeral head	Humeral external rotation
Subscapularis	SUBSC	Caudal half of scapula, in subscapular fossa, continuing around caudal margin	Minor tubercle of humerus	Humeral internal rotation
Teres major	TMJ	Caudal angle of the scapula	Crest of the lesser tubercle of the humerus	Humeral internal rotation
Teres minor	TMN	Above glenoid of scapula, continuing onto glenohumeral joint capsule/soft tissues	Lesser tubercle of humerus	Humeral internal rotation
Coracobrachialis longus	CB-L	Ventral aspect of coracoid	Ventral aspect of humerus, extending towards entepicondyle	Humeral adduction and flexion
Coracobrachialis brevis	CB-B	Ventral aspect of coracoid	Proximal ventral aspect of humerus	Humeral adduction and flexion
Biceps brachii longus	BI-L	Ventral aspect of epicoracoid, and an apparent second attachment on ventral coracoid	Unclear, tendon too long to mark but palpation of insertion suggests ulna	Draw scapulocoracoid laterally; Humeral adduction; Elbow flexion
Biceps brachii brevis	BI-B	Ventral aspect of coracoid	Small crest at proximal one-third of radius	Humeral adduction; Elbow flexion
Triceps brachii longus superficialis	TRI-LS	Spinous crest on the external aspect of the scapula	Olecranon of the ulna	Humeral abduction; Elbow extension
Triceps brachii longus profundus	TRI-LP	External aspect of scapula, above glenoid	Olecranon of the ulna	
Triceps brachii lateralis	TRI-L	Proximal dorsal aspect of the humerus, at the top of the linea dorsoventralis anterior	Anterior tubercle of olecranon of ulna	Elbow extension
Triceps brachii accessorius	TRI-A	Proximal dorsal aspect of humerus	Olecranon of ulna	
Triceps brachii medialis	TRI-M	Distal dorsal aspect of humerus	Posterior tubercle of olecranon of ulna	Elbow extension

body-mass normalized value was then calculated for each muscle (Supplementary Data file). Body mass-normalized parameters allowed broad comparisons to be made between species of different size (see below). Finally, these architectural parameters were also scaled to an echidna of body mass 3.31 kg, to contextualize architecture in real-world terms and match the mass of the contrast-stained specimen displayed in the gross musculoskeletal anatomy (Figs. 1, 2, 3, 4, and 5).

Body mass-normalized values of PCSA and fascicle length were compared to normalized muscle architecture parameters calculated from other published mammal species (Supplementary Data file): the fossorial mole *Scalopus aquaticus* (Rose et al. 2013), the fossorial badger *Taxidea taxus* (Moore et al. 2013), the cursorial hare *Lepus europaeus* (Williams et al. 2007), the arboreal pine marten *Martes martes* (Böhmer et al. 2018), and the terrestrial opossum *Didelphis virginiana* (Fahn-Lai et al., 2020). Additionally, parameters were compared with two sprawling non-mammals: the tegu lizard *Salvator merianae* (Fahn-Lai et al., 2020), and the alligator *Alligator mississipiensis* (Allen et al. 2014, Supporting Information Data S5 specimen LAA6). PCSA was re-calculated from the muscle belly masses, pennation angles, and muscle fascicle lengths reported in these studies, using Eq. 1, to ensure the same method and scaling was applied to all species. The mean value of each parameter was used from each animal, apart from the alligator, where data from an individual of similar mass to the 3D modeled echidna were used. Muscle architecture parameters were scaled by body

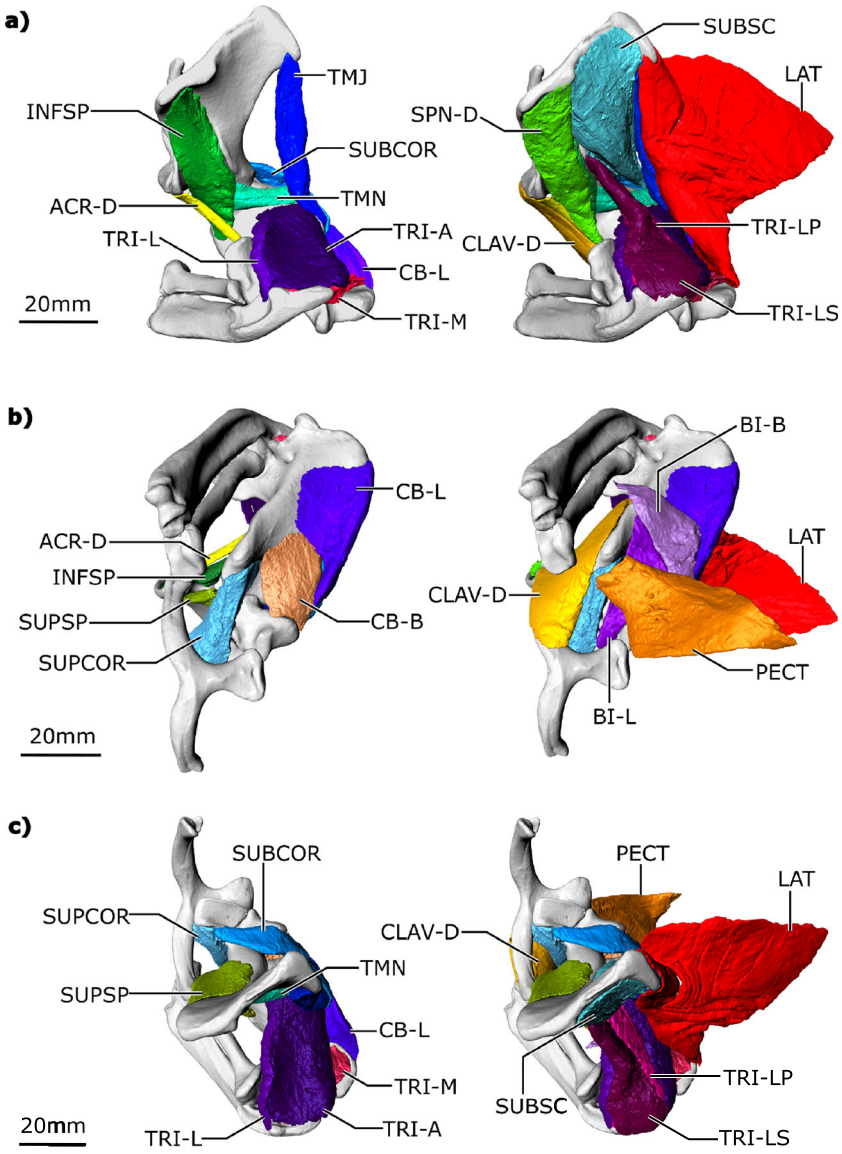

Fig. 2 Deep (left) and more superficial (right) contrast-stained and segmented shoulder muscle anatomy of the short-beaked echidna *Tachyglossus aculeatus* shown in **a**) left lateral view, **b**) ventral view, and **c**) dorsal view. For abbreviations see Table 1

mass reported in each study (mean body mass, and the reported mass for specimen LAA6 of Allen et al. 2014).

The R package 'dispRity' (Guillerme 2018) was used to compare variance in the mean body mass-normalized architectural parameters (fascicle length and PCSA) of the different species. The disparity metric is equivalent to the mean Euclidean distance between the observed muscle points and a 'centroid' (or mean point) on an x-y plot of PCSA vs. fascicle length. To capture the spread as well as the disparity of each species' muscle architecture, the interquartile range of observed muscle point distances to the centroid are also reported. The disparity metric is calculated as disparity between the single value (e.g., mean body-mass-normalised of PCSA/fascicle length) for each muscle of a species i.e., disparity between muscles.

All data generated or analyzed during this study are included in this published article (and its supplementary information files).

Results

Muscle Geometry

Differentiation of individual muscles via contrast-staining was generally good, despite relatively less diffusion of contrast agent to some very deep parts of the pectoral girdle muscles (e.g., the origin of m. subcoracoideus). For ease of description, muscles are classified here into functional groups inferred from estimates of glenohumeral muscle moment arms from a previous study (Regnault and Pierce 2018), but note that many muscles cross additional joints and/or have multiple inferred actions. As such, muscle functional group here is classified only according to the largest moment arm produced by that muscle at the glenohumeral joint. In addition to the figures referenced within, an interactive supplementary three-dimensional PDF is available online.

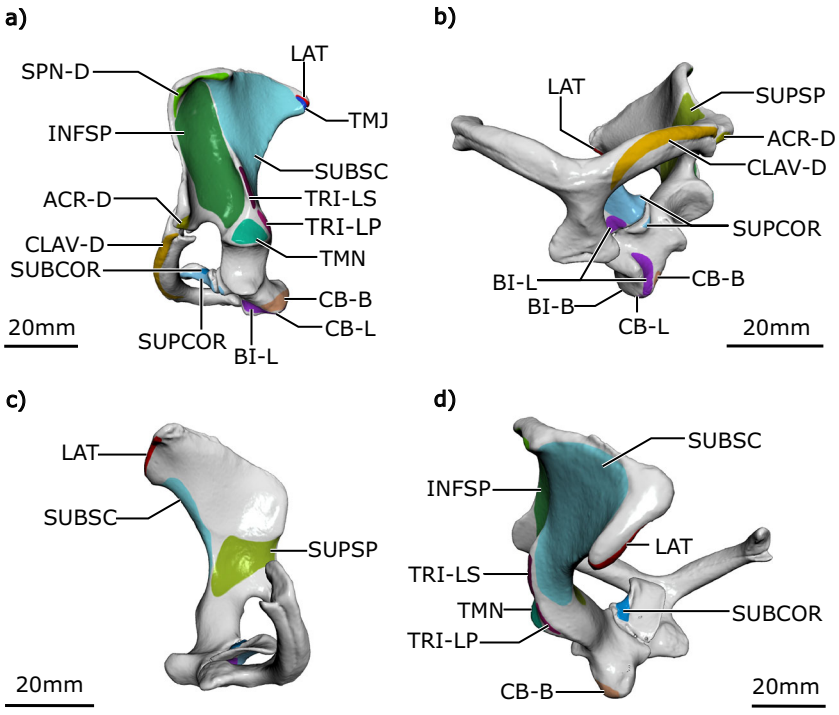

Fig. 3 Attachment sites of muscles highlighted in Fig. 2 on the echidna's left shoulder girdle bones (scapulocoracoid, clavicle-interclavicle, and epicoracoid), viewed from the animal's **a**) left lateral aspect, **b**) ventral aspect, **c**) medial aspect, and **d**) dorsal aspect. For abbreviations see Table 1

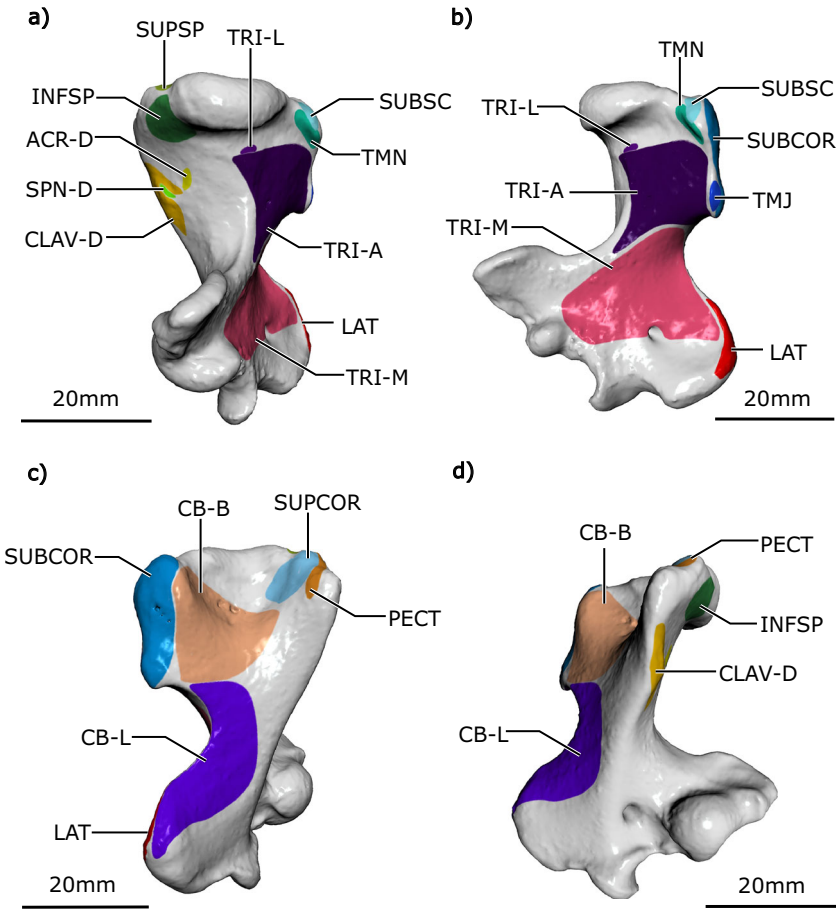

Fig. 4 Attachment sites of muscles highlighted in Fig. 2 on the echidna's left humerus, viewed from the bone's **a**) proximal dorsal aspect, **b**) distal dorsal aspect, **c**) proximal ventral aspect, and **d**) distal ventral aspect. For abbreviations see Table 1

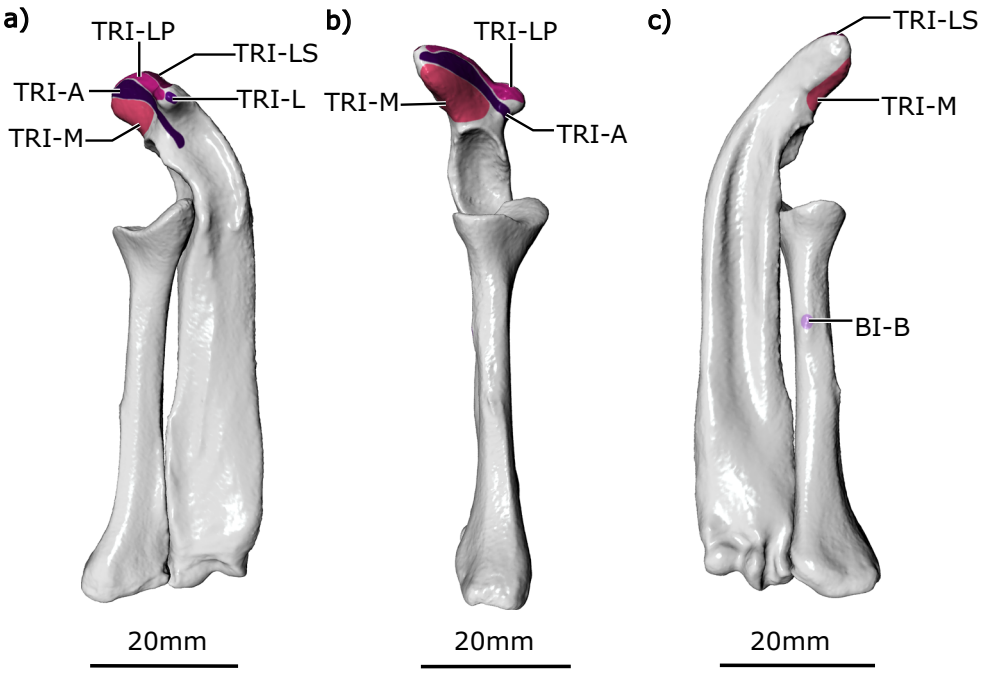

Fig. 5 Attachment sites of muscles highlighted in Fig. 2 on the echidna's left radius and ulna, viewed from animal's **a**) cranial aspect, **b**) preaxial aspect, **c**) caudal aspect. For abbreviations see Table 1

The humeral internal rotators originate and insert near one another. The m. latissimus dorsi (here abbreviated LAT and also called m. latissimus spinalis; Gambaryan et al. 2015) has a muscular origin from the caudal scapula (Fig. 3a-d) and vertebral column, with an aponeurotic extension caudally along the vertebral column, and inserts on the edge of the distal humeral entepicondyle (Fig. 4a-c). The m. teres major (TMJ) arises alongside the scapular origin of m. latissimus dorsi (Fig. 3a), and inserts proximally on the crest of the lesser tubercle of the humerus (Fig. 4b). The m. subscapularis (SUBSC) originates below these, in the subscapular fossa on the external caudal aspect of the scapula (Fig. 3a,c-d), and inserts on the lesser tubercle of the humerus (Fig. 4a-b). The m. teres minor (TMN) originates above the glenoid fossa (Fig. 3a), and also inserts on the lesser tubercle (Fig. 4a-b). Together, the humeral internal rotator group had the greatest combined muscle mass, principally through the bulky mm. latissimus dorsi and subscapularis.

The humeral external rotators, mm. supraspinatus (SUPSP) and infraspinatus (INFSP), originate cranially on the scapula (Fig. 3a-d). The m. infraspinatus originates from the external aspect, in the infraspinous fossa (separated from the subscapular fossa by the crest of m. triceps longus), while m. supraspinatus originates from the internal scapular surface. Both insert on the greater tubercle of the humerus (Fig. 4a, d). The m. clavodeltoideus (CLAV-D) also acts principally to externally rotate and extend the humerus; this muscle originates along the length of the clavicle's ventral surface (Fig. 3a-b), and inserts below the greater tubercle on the cranial aspect of the humerus (Fig. 3a, d).

Of the humeral abductors, m. acromiodeltoideus (ACR-D) originates from the acromion (Fig. 3a-b) and inserts on a small area on the dorsal aspect of the proximal humerus (Fig. 4a). This muscle appears to have a split or subdivision in the segmented scan and in dissected specimens. The m. spinodeltoideus (SPN-D) originates on the dorsal edge of the scapula (Fig. 3a) and, enveloped within m. clavodeltoideus, inserts near m. acromiodeltoideus on the humerus (Fig. 4a). The m. coracobrachialis is divided into a long and short head (CB-L and CB-B), which originate on the ventral aspect of the coracoid (Fig. 3a-b, d) and insert along the ventral aspect of the humerus (Fig. 4c-d). The scapular heads of m. triceps brachii longus (TRI-LS and TRI-LP) originate from a crest between the infraspinous and subscapular fossae on the external scapula (Fig. 3a, d). These two heads are joined by the accessory (TRI-A) and lateral (TRI-L) heads originating from the caudal aspect of the proximal humerus and the medial head (TRI-M) originating from the distal dorsal surface of the humerus (Fig. 4a-b). All five heads of m. triceps brachii insert on the olecranon process of the ulna (Fig. 5).

The m. supracoracoideus (SUPCOR) and both heads of m. biceps brachii (BI-B and BI-L) act to adduct the humerus; all originate from the ventral epicoracoid and coracoid (Fig. 3a-b). The m. biceps brachii brevis inserts on a small crest on the caudal/ventral aspect of the radius (Fig. 5c). The m. biceps brachii longus possesses a longer tendinous insertion and was difficult to trace precisely on the contrast-stained scans, but from dissections appeared to insert on the ulna. The m. supracoracoideus inserts on the ventral aspect of the humerus' greater tubercle (Fig. 4c).

The m. pectoralis (PECT) is usually considered a humeral adductor, although in the echidna its moment arms suggest it is capable of producing other equally forceful actions as a humeral internal rotator and extensor. The m. pectoralis is not subdivided; it originates along the presternum (=manubrium) and three sternal elements, and inserts next to m. supracoracoideus on the crest of the greater tubercle of the humerus (Fig. 4c-d).

The m. subcoracoideus (SUBCOR) appears to be the only muscle whose principal action is humeral flexion. This muscle originates on the internal surface of the epicoracoid (Fig. 3a, d) and inserts on the caudal humerus, along the lesser tubercle and crest of the lesser tubercle (Fig. 4b-c). None of the muscles examined here appear to act principally as humeral extensors (based on relative size of their moment arms), though several are capable of producing humeral extension alongside other movements, e.g., m. pectoralis, m. clavodeltoideus (above).

Muscle Architecture

Many of the muscles crossing the shoulder generally had little to no external tendon, attaching directly to bone or via short internal tendons or superficial aponeuroses. This can be seen in Fig. 2; the contrast agent is not taken up by dense connective tissues (tendon, ligament), so only muscle tissue is visible and can be seen in direct apposition with the bone. However, a few muscles did have an appreciable tendon, including m. spinodeltoideus (20 mm), m. biceps brachii longus and brevis (16 and 12 mm), and m. coracobrachialis longus (7 mm); see Table 2.

Many muscles appeared to have fascicles oriented parallel to the muscle's long axis, with fascicles running along much of the muscle's length. On closer examination, some of these muscles possessed fascicles inserting directly onto bone, but other fascicles elsewhere within the same muscle inserted at a slight angle onto short internal tendons or superficial aponeuroses (e.g., m. pectoralis and m. latissimus dorsi). Mean pennation angles from these muscles, calculated from angle measurements made at three different muscle regions, ranged from 2 to 13° (Table 2). Other muscles were clearly parallel-fibered throughout (m. acromiodeltoideus, m. biceps brachii longus, m. coracobrachialis brevis, m. supracoracoideus, m. teres minor, m. triceps medialis), with pennation angles of 0°. Finally, a third of the examined muscles were more clearly pennate, with mean pennation angles between 15 and 22° (m. coracobrachialis longus, m. infraspinatus, m. spinodeltoideus, m. subscapularis, m. supraspinatus, m. teres major, m. triceps brachii accessorius).

The spread of fascicle lengths and PCSAs among the echidna's shoulder muscles are shown in Fig. 6. Many of the

Table 2 Pectoral girdle and proximal limb muscle architectural properties of the short-beaked echidna *Tachyglossus aculeatus*. Values are the mean of each specimen, scaled to the body mass of specimen SEP42 (3.31 kg). Values scaled per gram of body mass are included in Supplemental Data file

Muscle	Muscle belly mass m_M (g)	Muscle belly length m_L (mm)	External tendon length (mm)	Pennation angle θ (°)	Fascicle length f_L (mm)	PCSA (mm^2)	f_L:m_L	PCSA:m_M
'humeral internal rotators'								
LAT	14.59	107	0	13	78	176.4	0.52	26.8
TMJ	2.25	55	1	19	38	47.1	0.71	33.6
SUBSC	6.18	63	1	16	33	165.5	0.73	12.1
TMN	0.83	25	0	0	22	16.4	0.88	19.8
'humeral external rotators'								
INFSP	2.06	52	1	17	30	55.6	0.80	23.0
SUPSP	1.54	37	1	22	24	57.4	0.86	36.8
CLAV-D	3.06	51	1	6	41	70.5	0.69	20.9
'humeral abductors'								
ACR-D	0.66	29	0	0	25	24.3	0.84	35.0
SPN-D	1.58	37	20	15	32	41.7	0.77	29.7
CB-L	3.82	53	7	19	32	111.0	0.77	24.8
CB-B	1.15	29	0	0	25	44.3	0.84	19.7
TRI-LS	2.13	53	0	11	38	47.1	0.70	32.1
TRI-LP	3.66	43	1	7	33	90.8	0.72	22.1
TRI-LAT	0.60	37	1	9	30	18.7	0.79	24.6
TRI-A	4.40	40	0	19	28	141.4	0.81	31.1
TRI-M	2.32	30	0	0	23	69.0	0.86	26.3
'humeral adductors'								
SUPCOR	0.78	31	0	0	26	27.3	0.81	17.4
BI-L	0.97	53	16	0	42	23.9	0.65	37.3
BI-B	1.77	59	12	11	48	31.4	0.58	27.0
PECT	4.78	55	0	2	46	94.4	0.60	29.1
'humeral flexors'								
SUBCOR	0.96	34	3	15	24	32.3	0.86	38.5

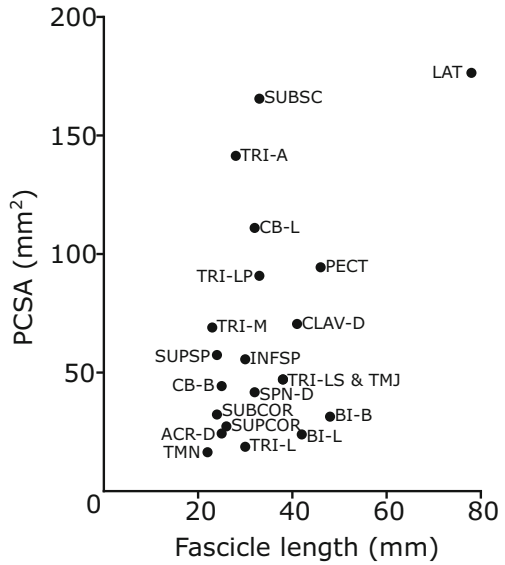

Fig. 6 Absolute architectural properties of echidna shoulder and proximal forelimb muscles (scaled to the 3.31 kg model specimen SEP42 from Regnault and Pierce 2018). For abbreviations see Table 1 and for muscle values see Table 2

muscles cluster around similar fascicle lengths, between approximately 20–45 mm, though m. latissimus dorsi can be clearly seen to possess the longest mean fascicle length at 78 mm. The long, near parallel structure of fascicles in many of the echidna's shoulder muscles, described above, is reflected in calculated ratios of fascicle length to muscle belly length (f_L:m_L Table 2, supplementary Fig. S1): for all muscles examined, fascicle lengths measured between 52 and 88% of total muscle belly length. Compared to fascicle length, the spread of PCSAs appears more diverse (Fig. 6). The muscles with the largest PCSAs were generally those with the largest masses (m. latissimus dorsi, m. subscapularis, the combined heads of m. triceps brachii, and the combined heads of m. coracobrachialis), though many of these muscles had some degree of fascicle pennation that would also have contributed toward increasing PCSA.

Comparison with Other Species

In general, the echidna shoulder muscles exhibited much less architectural variation compared with the other mammals (Fig. 7); few muscles had extremes of fascicle length and/or PCSA. Even muscles that appeared specialized in the echidna for large PCSA (e.g., m. subscapularis) or long fascicles (e.g., m. latissimus dorsi) (Fig. 6) did not approach the same body mass-normalized magnitudes as the other animals examined.

Analysis of architectural disparity between the species (Fig. 7b) shows the echidna to have the lowest observed disparity (0.72), followed by the tegu (0.97), alligator (1.07), badger (1.39), pine marten (1.47), opossum (1.63), hare (1.97), and mole (2.38).

Relative to each muscle's length and mass, the echidna possesses muscles with relatively long fascicles and small-to-intermediate PCSAs (Table 2, Supplementary Fig. S1). These values are similar to the range exhibited by tegu muscles (fascicles between 54 and 93%), and many of the mole muscles (fascicles between 63 and 100%, excluding mm. supraspinatus and infraspinatus). In contrast to the echidna, the alligator, opossum, hare, and pine marten muscles have more variable relative muscle fascicle lengths and PCSAs.

Discussion

The main aim of the study was to characterize the architecture of the shoulder and proximal forelimb muscles in the monotreme echidna, to better understand forelimb function and evolution in this relatively under-studied but phylogenetically important group of animals. We anticipated that the echidna would show muscle architectural specializations related to its lifestyle and locomotion. Namely, we hypothesized increased force-generating capacity (via large PCSA) for humeral internal rotators and adductors, which have been identified as important in the fossorial sprawling echidna in our previous study (Regnault and Pierce 2018), and would be convergent with other fossorial mammals (e.g., moles, Rose et al. 2013) and sprawling non-mammals (e.g., crocodilians, Allen et al. 2014).

Both echidnas (Monotremata: Tachyglossidae) and moles (Placentalia: Talpidae) are thought to be humeral rotation diggers (Hildebrand 1985; Kley and Kearney 2007). Although separated by long evolutionary distances they share some anatomical similarities, including a robust humerus with convergent 'hourglass' morphology (Weisbecker 2011), bulky pectoral girdle (Rose et al. 2013), and broad spade-like manus with restricted joint mobility (Hildebrand 1985). Many muscles appear to act similarly in the mole and echidna, particularly to produce internal humeral rotation (Regnault and Pierce 2018). Counter to our expectations, we found that echidna body mass-normalized muscle architecture parameters were not appreciably convergent to the mole or other fossorial mammals examined. Unlike the mole, m. teres major in the echidna appeared unremarkable in terms of PCSA (Table 2, Fig. 6). The m. subscapularis was relatively large and had larger PCSA than the other echidna shoulder muscles (Fig. 6), but even this muscle did not show the same extreme specialization relative to body mass as in the mole or badger (Fig. 7a, Supplementary Data file). The m. pectoralis was another muscle we anticipated might show architectural specialization (Regnault and Pierce 2018), due to its importance as a humeral adductor in sprawling animals. However, it also did not have large PCSA or long muscle fascicles relative to other muscles in the echidna shoulder (Table 2, Fig. 6) nor when compared with the pectoral muscle(s) of other sprawling and upright animals (Fig. 7, Supplementary Data file).

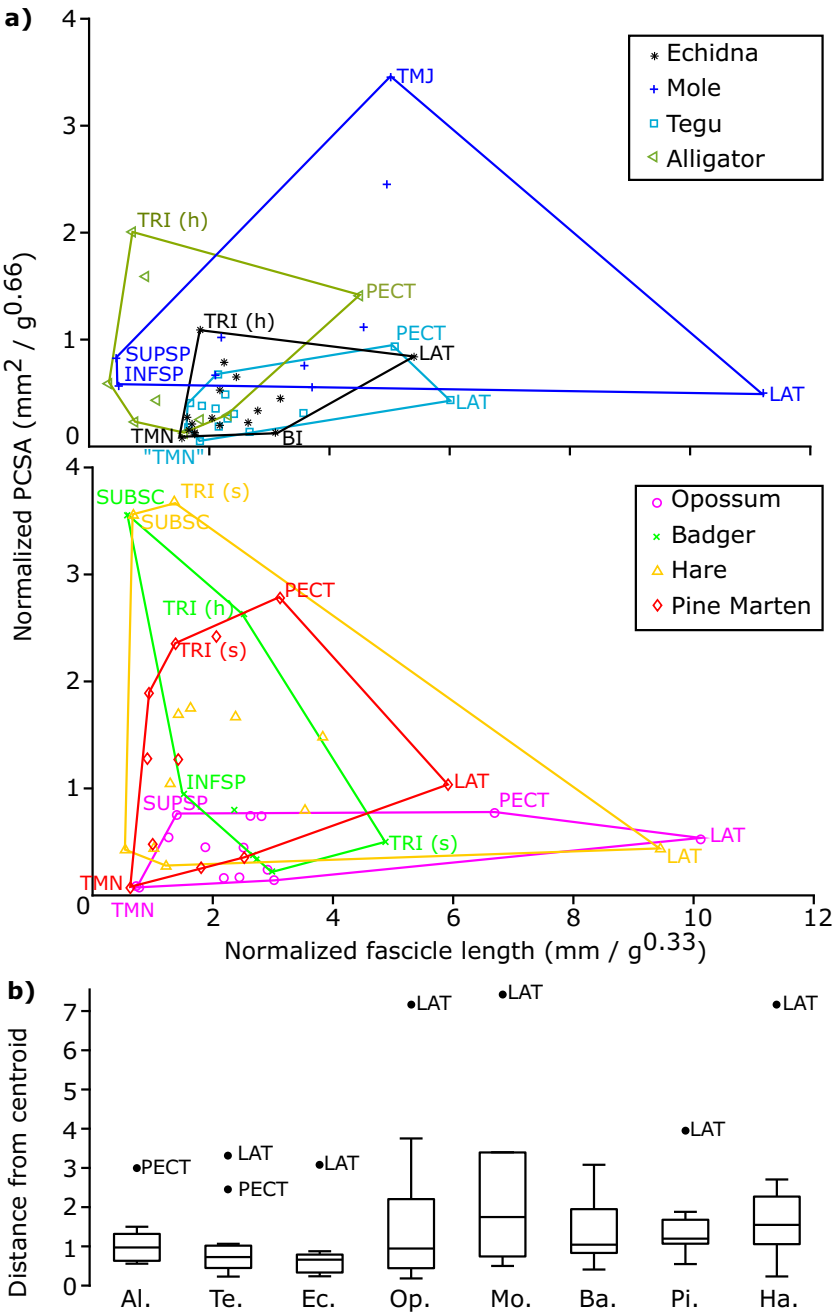

Fig. 7 **a**) Muscle architectural parameters, normalized by body mass in grams, for sprawling animals (echidna, mole, tegu, alligator) and non-sprawling therians (opossum, badger, hare, pine marten). See Materials and Methods for literature sources of data. Outlines show the range of each species, and selected muscles with extreme values are labeled. Note that the multi-headed m. triceps brachii has been grouped into scapular and humeral heads, labeled TRI(s) and TRI(h), and m. scapulohumeralis anterior of the tegu has been labeled TMN following its probable homology with m. teres minor; see Fahn-Lai et al. (2020). **b**) Boxplot illustrating muscle architecture disparity between species: the mean distance of each muscle to the centroid of the outlined area in part (a). Species abbreviations: Al. = alligator, Te. = tegu, Ec. = echidna, Op. = opossum, Mo. = mole, Ba. = badger, Pi. = pine marten, Ha. = hare. Data are provided in Supplementary Data file

In fact, the echidna's shoulder and proximal forelimb muscle architecture appears fairly unspecialized. PCSA and fascicle length values showed little spread, and measures of disparity placed the echidna lowest amongst all the animals compared here, closest to the tegu lizard than to any of the other mammals (Fig. 7a-b). Of all the echidna muscles examined, m. latissimus dorsi was probably the most divergent, with the longest mean fascicle length and one of the largest PCSAs (Figs. 6, 7b). This is likely linked to the muscle's overall anatomy: m. latissimus dorsi inserts very distally on the humerus in monotremes compared with other animals (Gambaryan et al. 2015). Even so, its mean fascicle length does not reach the same extremes as m. latissimus dorsi in the hare, opossum, or mole, and neither is its PCSA especially notable when considered against the range of muscle PCSAs exhibited by other animals (Fig. 7). In contrast to the echidna, all other mammals examined here showed much more variation in shoulder muscle PCSAs and fascicle lengths, with the mole exhibiting the greatest disparity. The muscle parameters used in the calculation of disparity are scaled by body mass, so in part, increased disparity (e.g. mole, hare) can be a reflection of an increase in the proportion of the measured forelimb

muscle masses (5.4% and 3.4% of body mass in the mole and hare, respectively, compared to 1.8% in the echidna – see Supplementary Data file). In these cases, increased disparity results from some forelimb muscles maintaining similar relative mass, while there are dramatic increases in masses of other specific and apparently functionally-relevant muscles (e.g., m. teres major and m. pectoralis in the mole, m. triceps brachii and m. pectoralis in the hare). The latter appear to be driving the relative increase in overall forelimb muscle mass (the two muscles in each example accounting for over 55% of measured forelimb muscle mass for those species).

When architectural parameters are expressed relative to each muscle's size (Supplementary Fig. S1), another pattern then emerges. In terms of muscle architecture relative to muscle size, the echidna (and tegu) again shows little variation. Moles are more variable; however, this appears to be mostly driven through modulation of muscle size. Once muscle size is accounted for, many mole muscles have similar relative f_L and PCSA as in the echidna. By referring to Eq. (1), we can see that pennation angle and fascicle length become the determinants of PCSA:m_M – and of these, fascicle length appears to be the primary source of diversity. Muscle pennation can help to pack in more short fibers/fascicles (Gans 1982), but does not appear a prerequisite for achieving high PCSA:m_M, e.g., the m. coracobrachialis in the alligator has one of the highest PCSA:m_M and no pennation. The echidna shows only a 3.5-fold difference between its shortest and longest f_L; tegus are similar at 3.6, and moles 5.3 (when excluding mm. supraspinatus and infraspinatus, as discussed below). In contrast, the other therian mammals and the alligator show much greater variation in fascicle length (up to 17.5x in the hare), and consequently much more variation in both f_L:m_L and PCSA:m_M.

Why are the echidna shoulder muscles so architecturally similar? Perhaps muscle specializations are unnecessary. Muscles with short fascicles in highly pennate arrangements, with large resultant PCSAs, are capable of generating large forces but do not shorten much; these muscles are inferred to have specialized roles as joint stabilizers (Lieber and Fridén 2000; Rose et al. 2013; Moore et al. 2013). Examples include mm. supraspinatus and infraspinatus in therian mammals (Fig. 7, Supplementary Fig. S1). These stabilizing muscles are important in therians, to compensate for their highly mobile pectoral girdle and glenohumeral joints (Luo 2015). However, the echidna (like earlier mammaliaforms; Luo 2015) has less mobility at the scapula and glenohumeral joint; the robust and interlocking bones and joint morphologies of the echidna's pectoral girdle and forelimb may explain why its muscles have not acquired 'stabilizer' muscle architecture. Relative to muscle size, the echidna's muscles instead have long fascicles and small-to-moderate PCSAs (similar to the tegu lizard). Such muscles are capable of relatively greater and more rapid shortening, and are suited for force production over a wide range of the muscle's range of motion (Rose et al. 2013). The echidna's low architectural diversity can thus be interpreted as a lack of muscle specialization into distinct roles (e.g., joint stabilizing, or high force production over narrow working ranges for specific movements), and/or a generalized need for muscles with wide working ranges (e.g., potentially as an adaptation for fossoriality; Rose et al. 2013).

It is notable that muscle architectural parameters in the echidna appear to be broadly conservative. Extant mammals – and particularly eutherians (placentals) – exploit a huge variety of ecological niches and locomotory strategies, underpinned by modifications of their forelimb into fins, wings, and other specialized structures (Polly 2007; Kelly and Sears 2011). The wide variety of PCSAs and fascicle lengths exhibited by the eutherian shoulder muscles sampled thus far suggests that the remarkable versatility of the placental forelimb extends to the level of muscle architecture. Metatherians (marsupials) appear more constrained in forelimb versatility, perhaps because their forelimb structure is linked to their reproductive strategy of climbing to the pouch after birth (e.g. Kelly and Sears 2011; but see Martín-Serra and Benson 2019). Although we examined data from only one marsupial in our study (the opossum), its muscle architecture parameters are less diverse than the eutherian mammals, and so appear to reflect the generalized constraint on marsupial forelimb anatomy. Although monotremes possess a mosaic of plesiomorphic and more derived forelimb anatomical features, no developmental constraints of the forelimb have been identified comparable to marsupials, and so monotremes might be expected to exhibit more muscle architectural diversity than the echidna does here.

If the echidna's architecture does indeed reflect lack of muscle specialization into distinct roles (rather than reflecting a fossorial lifestyle, as discussed above), one possibility may be that diversification of mammalian muscle architecture occurred in the lineage leading to stem therians or eutherians, after their divergence from monotremes, alongside increased diversification of the forelimb more generally. Fahn-Lai et al. (2020) offered evidence that the architecture of many homologous shoulder muscles is statistically similar between tegu lizards and opossums. They interpreted the surprising similarity in functional characteristics as either conservation from the amniote state or convergence towards a small-bodied ecological generalist phenotype, and link differences to a postural shift from 'sprawling' to 'parasagittal' limb posture and movement in therians. Though we do not directly compare homologous muscles in this study, we note that the echidna, phylogenetically bracketed by those two species, also appears to support the notion of conserved muscle architecture in terms of overall diversity. We found the spread of echidna muscle architecture values closest to the tegu, which might be expected given that monotremes diverged from other mammals prior to the hypothesized acquisition of parasagittal posture (Kielan-Jaworowska and Hurum 2006).

In conclusion, we find that the muscle architecture of the echidna pectoral girdle and proximal forelimb is functionally conservative. Muscle PCSAs and fascicle lengths do not appear modified for specific roles (e.g., stabilization) to the same extent as in other fossorial mammals, or indeed any of the other animals sampled apart from the tegu. Rather, all the echidna's muscles show similar relative architectural parameters, suited for low-to-moderate force production over a wide working muscle range. Our species comparisons using existing literature data also suggest that the increase in diversity in eutherian forelimb structure and function may be mirrored by increasing disparity of muscle architecture in these species, though more data are needed to test this. Diversity in muscle architecture in the studied species appears to be primarily driven through modulation of effective fascicle length (and in some cases, relative muscle size). Muscle architectural studies such as ours are therefore of key importance, not only for better understanding forelimb function in extant animals like the echidna and other mammals, but also for their contribution to reconstructing function in extinct taxa (Bates and Falkingham 2018; Regnault and Pierce 2018; Fahn-Lai et al. 2020).

Acknowledgements We thank Anthony Wilkes (The University of Adelaide) for specimen acquisition, Katrina Jones (Harvard University) for CT scanning advice, Blake Dickson (Harvard University) for guidance in implementing R analyses, and the Pierce Lab for discussions while performing this research. We also thank John R. Wible, Karl T. Bates, and one anonymous reviewer for helpful comments on a previous version of this manuscript. This project was supported by the National Science Foundation grant no. DEB-1754459 and EAR-1524523 to S.E.P.

Author Contributions S.E.P. and S.R. conceived and designed the project. S.R. collected the echidna data and P.F-L. collected the tegu and opossum data. R.M.N. collected the echidna specimens. S.R. analyzed the data and made all figures, tables, and supplementary files. S.R. and S.E.P. drafted the manuscript. All authors edited the manuscript and gave final approval for publication.

Compliance with Ethical Standards

Competing Interests The authors declare that they have no competing interests.

References

Allen V, Elsey RM, Jones N, Wright J, Hutchinson JR (2010) Functional specialization and ontogenetic scaling of limb anatomy in *Alligator mississippiensis*. J Anat 216(4):423–445

Allen V, Molnar J, Parker W, Pollard A, Nolan, G, Hutchinson JR (2014) Comparative architectural properties of limb muscles in Crocodylidae and Alligatoridae and their relevance to divergent use of asymmetrical gaits in extant Crocodylia. J Anat 225(6): 569–582

Augee ML, Gooden B, Musser A (2006) Echidna: Extraordinary Egg-laying Mammal. CSIRO Publishing, Canberra

Bates KT, Falkingham PL (2018) The importance of muscle architecture in biomechanical reconstructions of extinct animals: a case study using *Tyrannosaurus rex*. J Anat 233(5):625–635

Böhmer C, Fabre AC, Herbin M, Peigné S, Herrel A (2018) Anatomical basis of differences in locomotor behavior in martens: a comparison of the forelimb musculature between two sympatric species of *Martes*. Anat Rec 301(3):449–472

Clemente CJ, Cooper CE, Withers PC, Freakley C, Singh S, Terrill P (2016). The private life of echidnas: using accelerometry and GPS to examine field biomechanics and assess the ecological impact of a widespread, semi-fossorial monotreme. J Exp Biol 219(20):3271–3283

Fahn-Lai P, Biewener AA, Pierce SE (2020) Broad similarities in shoulder muscle architecture and organization across two amniotes: implications for reconstructing non-mammalian synapsids. PeerJ 8: e8556 https://doi.org/10.7717/peerj.8556

Gambaryan PP, Kuznetsov AN (2013) An evolutionary perspective on the walking gait of the long-beaked echidna. J Zool 290(1):58–67

Gambaryan PP, Kuznetsov AN, Panyutina AA, Gerasimov SV (2015) Shoulder girdle and forelimb myology of extant Monotremata. Russ J Theriol 14(1):1–56

Gans C (1982) Fiber architecture and muscle function. ESSR 10(1):160–207

Gignac PM, Kley NJ, Clarke JA, Colbert MW, Morhardt AC, Cerio D, Cost IN, Cox PG, Daza JD, Early CM, Echols MS (2016) Diffusible iodine-based contrast-enhanced computed tomography (diceCT): an emerging tool for rapid, high-resolution, 3-D imaging of metazoan soft tissues. J Anat 228(6):889–909

Guillerme T (2018) dispRity: a modular R package for measuring disparity. Methods Ecol Evol 9(7):1755–1763

Hildebrand M (1985) Digging of quadrupeds. In: Hildebrand M, Bramble DM, Liem KF, Wake DB (eds) Functional Vertebrate Morphology. Harvard University Press, Cambridge, pp 89–109

Jenkins FA Jr (1970) Limb movements in a monotreme (*Tachyglossus aculeatus*): a cineradiographic analysis. Science 168(3938):1473–1475.

Jouffroy FK, Lessertisseur J (1971) Musculature post-cranienne. In: Grassé P-P (ed) Traite de Zoologie, Tome XVI (Fascicle III). Masson, Paris, pp 733–836

Kelly EM, Sears KE (2011) Limb specialization in living marsupial and eutherian mammals: constraints on mammalian limb evolution. J Mammal 92(5):1038–1049

Kielan-Jaworowska Z, Hurum JH (2006) Limb posture in early mammals: sprawling or parasagittal. Acta Palaeontol Pol 51(3):393–406

Kley NJ, Kearney M (2007) Adaptations for digging and burrowing. In: Hall BK (ed) Fins into Limbs: Evolution, Development, and Transformation. University of Chicago Press, Chicago, pp 284–309

Lieber RL, Fridén J (2000) Functional and clinical significance of skeletal muscle architecture. Muscle Nerve 23(11):1647–1666

Lin YF, Konow N, Dumont ER (2019) How moles destroy your lawn: the forelimb kinematics of eastern moles in loose and compact substrates. J Exp Biol 222(4):jeb182436

Luo ZX (2015) Origin of the mammalian shoulder. In: Dial KP, Shubin N, Brainerd EL (eds) Great Transformations: Major Events in the History of Vertebrate Life. University of Chicago Press, Chicago, pp 167–187

Martín-Serra A, Benson RBJ (2019) Developmental constraints do not influence long-term phenotypic evolution of marsupial forelimbs as revealed by interspecific disparity and integration patterns. Am Nat https://doi.org/10.1086/707194

Méndez J, Keys A (1960) Density and composition of mammalian muscle. Metabolism 9:184–188

Moore AL, Budny JE, Russell AP, Butcher MT (2013) Architectural specialization of the intrinsic thoracic limb musculature of the American badger (*Taxidea taxus*). J Morphol 274(1):35–48

Polly PD (2007) Limbs in mammalian evolution. In: Hall BK (ed) Fins into Limbs: Evolution, Development and Transformation. University of Chicago Press, Chicago, pp 245–268

Regnault S, Pierce SE (2018) Pectoral girdle and forelimb musculoskeletal function in the echidna (*Tachyglossus aculeatus*): insights into mammalian locomotor evolution. R Soc Open Sci 5(11):181400

Rose JA, Sandefur M, Huskey S, Demler JL, Butcher MT (2013) Muscle architecture and out-force potential of the thoracic limb in the eastern mole (*Scalopus aquaticus*). J Morph 274(11):1277–1287

Schneider CA, Rasband WS, Eliceiri KW (2012) NIH image to ImageJ: 25 years of image analysis. Nat Methods 9(7):671

Weisbecker V (2011) Monotreme ossification sequences and the riddle of mammalian skeletal development. Evolution 65(5):1323–1335

Williams SB, Wilson AM, Payne RC (2007) Functional specialisation of the thoracic limb of the hare (*Lepus europeus*). J Anat 210(4):491–505